Journal of
Ceramic Science
and Technology

J. Ceram. Sci. Tech., 07 [01] 65-70 (2016)
DOI: 10.4416/JCST2015-00028
available online at: http://www.ceramic-science.com

Synthesis and *in vitro* Bioactivity Mechanism of Synthetic α-wollastonite and β-wollastonite Bioceramics

R. Morsy*, R. Abuelkhair, T. Elnimr

Biophysics Lab, Physics Department, Faculty of Science. Tanta University, Tanta 31527, Egypt
received June 23, 2015; received in revised form August 26, 2015; accepted September 30, 2015

Abstract

Synthetic wollastonite ceramics have received great attention as promising bioceramics for enhancing the properties of bone substitutes. However, uncertainty remains about the differences in bioactivity between its phases, that is α-wollastonite and β-wollastonite, and about the mechanism for inducing bone-like hydroxyapatite (b-HAp). In the present study, α-wollastonite and β-wollastonite ceramics were prepared with the co-precipitation method. For the *in vitro* bioactivity test, α-wollastonite and β-wollastonite powders were soaked in simulated body fluid (SBF) solution for 1, 2, 3, 4, 10 days. Synthetic α-wollastonite, β-wollastonite and induced b-HAp particles were characterized by means of XRD, FT-IR, SEM and electron spin resonance (ESR). The results showed significant differences in the bioactivity between the α-wollastonite and β-wollastonite samples; the β-wollastonite showed a significant increase in the rate of formation of b-HAp compared to that of α-wollastonite. ESR data showed a high sensitivity to study the formation process of b-HAp, and confirmed the role of defects in bioactivity mechanism. The bioactivity mechanism was observed to involve a dissolution process of the wollastonite and formation process of the b-HAp. Therefore, these results describe the *in vitro* bioactivity differences between α-wollastonite and β-wollastonite powders, emphasizing the importance of controlling their bioactivity parameter for developing bone biocomposites.

Keywords: Bioceramics, wollastonite, hydroxyapatite, precipitation, electron resonance

I. Introduction

Wollastonite ($CaSiO_3$) ceramics have attracted tremendous fundamental and medical interest on account of their properties as a reinforcing and improving agent for bioceramics and biopolymers used for bone repair applications [1–2]. The wollastonite has two polymorphic forms of calcium silicate ceramics with different structures and properties: β-wollastonite, a low-temperature phase synthesized at a temperature below 1125 °C and belonging to the triclinic crystal system, and α-wollastonite, a high-temperature phase synthesized at a temperature above 1125 °C, belonging to the monoclinic crystal system 3 – 4. As biomaterials, wollastonite ceramics exhibit excellent biological properties such as nontoxicity, biocompatibility, bioresorbability and bioactivity [5–6]. In addition, they enhance the mechanical and biodegradation properties of artificial bioceramics and biopolymers composites [7]. Various studies on the bioactivity of wollastonite ceramics have demonstrated their good ability to induce new apatite and bone formation more rapidly than other conventional bioglass and glass ceramics [8–11]. However, studies comparing the bioactivity of α-wollastonite and β-wollastonite and concerning the mechanism of inducing bone-like hydroxyapatite (b-HAp) are still limited. In bone repair and regeneration, bioactivity plays a key role in the selection of biomaterials that can bond to bone and induce new b-HAp formation [12]. Previous studies have confirmed the important role of silicon as active calcification sites in enhancing the activity of osteoblast cell and the formation of b-Hap [13–14]. Nevertheless, the differences between the bioactivity of α-wollastonite and β-wollastonite ceramics and the mechanism of inducing b-HAp are complex and not fully understood. Several studies have reported that the mechanism of bioactivity is strongly dependent upon various parameters: the parameters belonging to the ceramics such as their surface chemistry, morphology, defect structures, and grain size; and the parameters belonging to the surrounding medium such as its temperature, composition, and pH [15–19]. The commonly proposed mechanism that describes the ability of calcium silicates compounds to induce b-HAp in the physiological environment or SBF solution is complex and depends strongly on its surface chemistry [15]. The mechanism is based on various phases and steps; the surrounding solution can hydrate silica (SiO_2) on the ceramic surface, forming a hydrated surface layer of silanol (≡Si-OH) that absorbs calcium, phosphate, carbonate ions and anions from the surrounding solution. This provides the nucleation sites for precipitation of an amorphous calcium phosphate film on the silica-rich layer, which then crystallizes to form b-Hap [20–22]. Also, the composition of the SBF solution contains various anions and cations that can be entrapped in the HAp lattice during HAp formation and can facilitate the formation of free radicals, paramagnetic centers and defect centers in the nucleated HAp during the

* Corresponding author: r.morsy@science.tanta.edu.eg

soaking time [23]. The electron spin resonance (ESR) technique is a very sensitive method for detecting the free radicals and paramagnetic centers incorporated into material crystals [24]. Study of the *in vitro* bioactivity is essential to improve and enhance the bioactivity of wollastonite ceramics and their composites, so in the present study, ESR spectroscopy was used along with conventional methods such as X-ray diffraction (XRD), Fourier transform infrared spectroscopy (FT-IR), and scanning electron microscopy (SEM) to compare the bioactivity processes in α-wollastonite and β-wollastonite bioceramics. This work demonstrates that α-wollastonite and β-wollastonite exhibit qualitatively different bioactivity.

II. Experimental Methods

(1) Synthesis of the wollastonite powders

The α-wollastonite and β-wollastonite powders were synthesized with a co-precipitation method using an analytical grade $Ca(NO_3)_2.4H_2O$ and $Na_2SiO_3.9H_2O$ (Adwic, El-nasr Chemical Co., Cairo, Egypt). 0.1 moles of $Ca(NO_3)_2{\cdot}4H_2O$ and $Na_2SiO_3{\cdot}9H_2O$ were dissolved in 200 ml of aqua solution. $Ca(NO_3)_2{\cdot}4H_2O$ solution was added to the $Na_2SiO_3{\cdot}9H_2O$ solution under magnetic stirring. Then the container containing the solution was heated to 100 °C for 2 h. The precipitate was washed three times with distilled water, filtered, and dried overnight at 100 °C. To obtain β-wollastonite phase, the powder was calcined at 800 °C for 2 h, whereas for α-wollastonite phase, the powder was calcined at 1200 °C for 2 h.

(2) In-vitro bioactivity testing

The *in vitro* bioactivity of the α-wollastonite and β-wollastonite powders was assessed in a SBF solution with ion concentrations nearly equal to human blood plasma [23] . The ionic concentrations of this SBF are 142.0 mM Na^+, 5.0 mM K^+, 1.5 mM Mg^{2+}, 2.5 mM Ca^{2+}, 147.8 mM Cl^-, 4.2 mM HCO_3^{2-}, 1.0 mM HPO_4^{2-}, and 0.5 mM SO_4^{2-}. Tris-HCl served as a buffer to maintain a constant pH value of 7.4. The synthesized powders were placed in polyethylene bottles containing SBF maintained at 37.0 °C for 1, 2, 3, 4, 10 days before they were taken out for testing and analysis. The soaking was conducted in a liquid/solid ratio of 0.6 ml/mg in a shaking water bath without refreshing the soaking medium. After soaking, these samples were collected from the SBF solutions, rinsed with acetone and air-dried at room temperature.

(3) Sample characterization

The α-wollastonite and β-wollastonite samples, before and after soaking in SBF solution, were characterized with conventional methods. The structure of the α-wollastonite and β-wollastonite samples was characterized by means of x-ray powder diffraction (XRD) using a Philips PW 1840 diffractometer. CuK_α radiation of 1.5406Å wavelength at 40 kV and 30 mA was used to expose the samples through a Ni filter. The 2θ values were set in the range of 10 to 65° where almost all significant peaks of α-wollastonite , β-wollastonite and HAp crystals appeared. Peaks on the x-ray patterns recorded for the α-wollastonite and β-wollastonite samples before and after soaking were compared with the standard XRD pattern of β-$CaSiO_3$ (JCPD 84 – 0654), α-$CaSiO_3$ (JCPD 74 – 0874), and HAp (JCPD 09 – 0432). Fourier transformed infrared (FT-IR) spectra were obtained with Perkin-Elmer-1600 using a KBr pellet technique for the range 4 000 to 400 cm^{-1}. The microstructure of the samples was examined by means of scanning electron microscopy (SEM) using a JEOL 6400 electron microscope at 30 kV of electron acceleration voltage. ESR analyses were performed using a Bruker Elexys.500 (Band X) spectrometer at a microwave frequency of 9.71 GHz, a microwave power of 20 mW, power attenuations of 5 dB, a magnetic field of 100 – 500 mT, field modulation of 1.0 mT in amplitude and a modulator frequency of 100 kHz. The 1, 1 diphenyl 2-picryl hydrazyl (DPPH) was used as a standard reference material for the g-value. The g-value can be calculated according to Eq. (1)[25]:

$$g = 71.448 \frac{\nu\,(\text{inGHz})}{B\,(\text{in mT})} \qquad (1)$$

Where ν is the microwave frequency and B is the intensity of applied magnetic field.

III. Results and Discussion

The XRD patterns of synthetic α-wollastonite and β-wollastonite powders calcined at 800 and 1200 °C are shown in Fig. 1a (0d) and Fig. 1b (0d) respectively. As compared to JCPDS cards, it can be seen that the main component of the α-wollastonite and β-wollastonite samples is a pure phase. The sharp peaks indicated a high crystallinity. Fig. 1 shows the comparison of XRD spectra of α-wollastonite and β-wollastonite before and after soaking for various periods in the SBF solution. It can be noticed that with an increase in the soaking period, the relative intensity ratio of the peaks corresponding to α-wollastonite and β-wollastonite decreased whereas the b-HAp peaks increased. The b-HAp phase was detected at a peak of $2\theta = 31.7°$ for β-wollastonite powders soaked in SBF for two days (Fig. 1.a) and was detected after 10 days for α-wollastonite powders (Fig. 1.b). The b-HAp peaks were broad, resulting from the superfine and amorphous b-HAp granules. After 10 days, the β-wollastonite phase had completely disappeared compared to α-wollastonite phase, and was replaced by amorphous b-HAp. It is possible that silicon leaves the calcium silicate phases and is released into the SBF solution as soluble hydroxyl groups [26]. As shown in Fig. 1 (a and b), dashed line, the XRD patterns demonstrated that the manifested 211 reflection is attributed to b-HAp. Also, by comparing the relative peak intensity of β-wollastonite and b-HAp peak with that of α-wollastonite and b-HAp peak, it is deduced that the β-wollastonite phase was much more degradable into the SBF solution than the α-wollastonite phase. Therefore, the data showed that β-wollastonite samples exhibit more significant degradation and rapid formation of b-HAp than α-wollastonite samples.

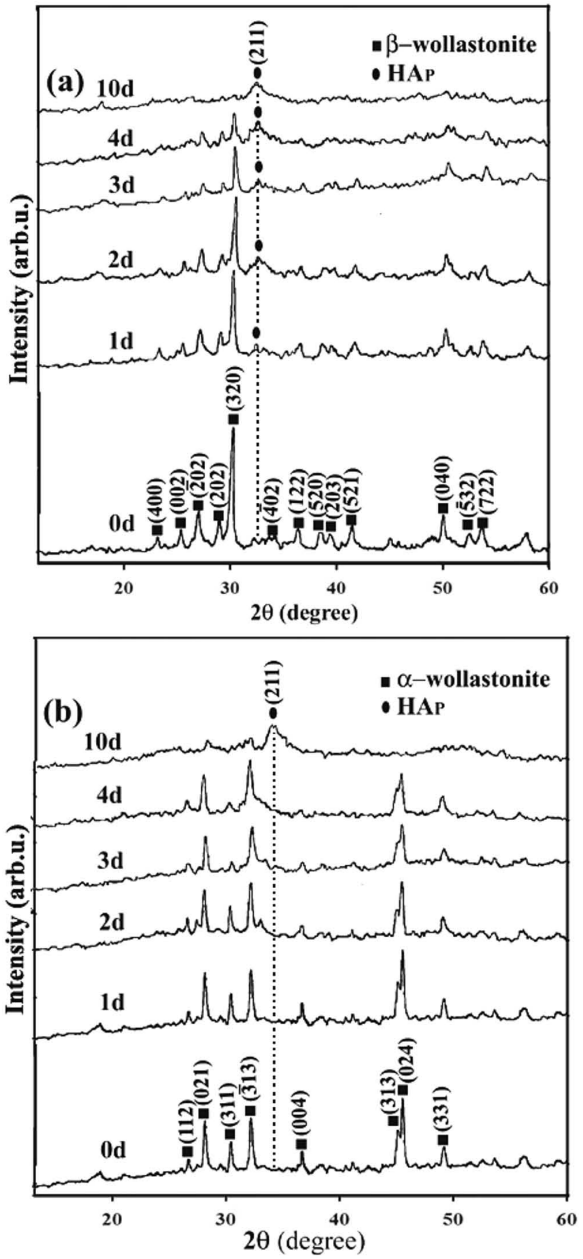

Fig. 1: XRD patterns of (a) β-wollastonite and (b) α-wollastonite powders after soaking in SBF for 0, 1, 2, 3, 4, 10 days.

Fig. 2 presents the FT-IR spectra of the α-wollastonite and β-wollastonite samples after they had been soaked in SBF for 0, 1, 2, 3, 4 and 10 days. The samples showed strong absorption at 1050 and 800 cm^{-1}, which was attributed to the Si-O stretching vibration. The band nears 450 cm^{-1}, which was due to the Si-O bending mode [27–28]. It was noted that the bands representing Si-O decreased with the increase in soaking time, indicating degradation of the samples. The bands at 645, and 567 cm^{-1} could be assigned to the phosphate group (PO_4^{-3}) of b-Hap [29], which appear with the β-wollastonite samples at 4 days and appeared at 10 days for α-wollastonite samples. FT-IR data are consistent with the XRD data, Fig. 1, where β-wollastonite induces formation of b-HAp more rapidly than the α-wollastonite samples. The data reveal that the formation of b-HAp layer did not prevent degradation of sintered wollastonite crystals. Also, the XRD and FT-IR data suggested that the dissolution and degradation of wollastonite induce and increase the formation of b-HAp. These results confirm the significance of the dissolution of wollastonite for the *in vitro* bioactivity of Ca-Si bioceramics.

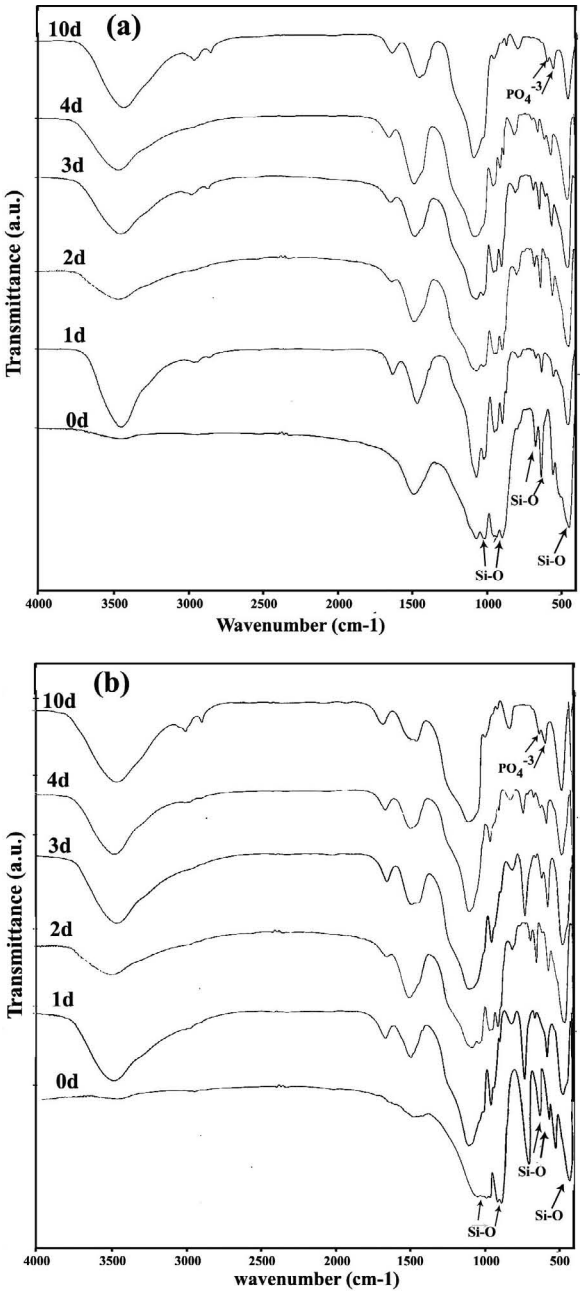

Fig. 2: FT-IR spectra of (a) β-wollastonite and (b) α-wollastonite powders after soaking in SBF for 0, 1, 2, 3, 4, and 10 days.

Fig. 3 shows the SEM images of the surface of α-wollastonite and β-wollastonite before and after soaking in SBF solution for 0, 3, and 10 days. It was found that after immersion for 3 days, β-wollastonite samples were completely covered by a layer of superfine amorphous b-HAp granules. In the case of the α-wollastonite samples, the surface was not completely changed. When the soaking time increased to 10 days, the surface layer of β-wollastonite samples became dense and b-HAp particles appeared agglomerated and crystallized whereas the α-wollastonite samples were still covered with an amorphous layer of superfine b-HAp particles. The SEM images show absence of induced needle-like HAp crystallites. The SEM data are con-

sistent with the XRD and FT-IR data, Figs. 1 and 2, where β-wollastonite induces formation of b-HAp more rapidly than α-wollastonite samples.

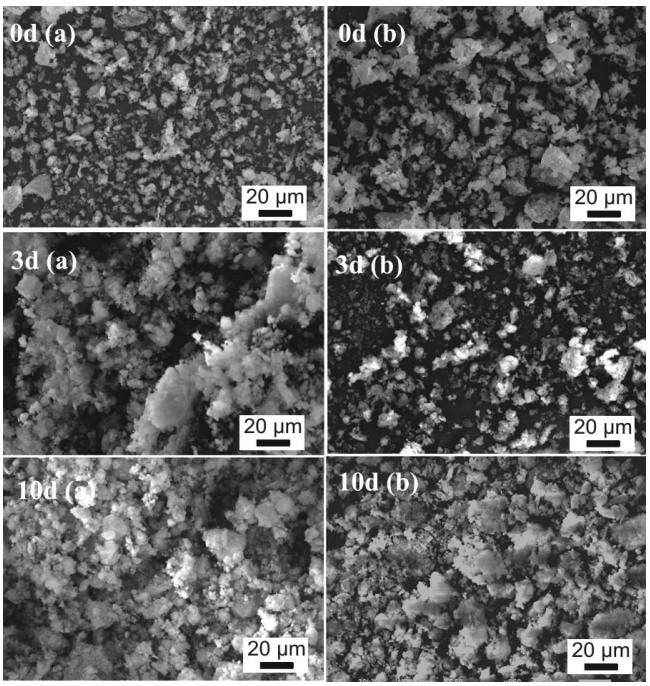

Fig. 3: SEM images of the surfaces of (a) β-wollastonite and (b) α-wollastonite samples soaked in SBF for 0, 3, 10 days.

Because the g-value of a radical is quite sensitive to the chemical environment of the unpaired electron, ESR spectra parameters of the g-value and ESR intensity of all the α-wollastonite and β-wollastonite powders before and after they had been soaked in SBF solution for 1, 2, 3, 4, and 10 days were studied. Table 1 shows obvious differences in the ESR signals behavior of the α-wollastonite and β-wollastonite powders before and after the samples were soaked in the SBF solution. Before the samples were soaked in the SBF solution, the α-wollastonite and β-wollastonite powders exhibited an ESR spectrum of g = 1.9737 and g = 1.9459 respectively. The values of ESR intensity for the α-wollastonite and β-wollastonite powders are 2600 and 2000 respectively, which are an adequate measure of the total amount of paramagnetic centers in the samples. These signals are attributed to $SiO^{\cdot}$ paramagnetic centers [30]. The difference in the value of g-factor is due to the effects of heating, phase transformation and increasing in grain size [31].

After soaking for one day, the β-wollastonite samples exhibited a large change in the g-value from 1.9737 to 1.8926 and a decrease in ESR intensity from 2600 to 1900, whereas the α-wollastonite exhibited a change from 1.9459 to 1.8926 and an increase in ESR intensity from 2000 to 2600. These variations indicate the changes in chemical environment and type of radicals incorporated in the α-wollastonite and β-wollastonite structures. The SBF solution is known to contain ions responsible for the formation of b-HAp on the surface of soaked powder; it induces paramagnetic centers that are responsible for the ESR spectrum [23]. The equality of the g-value for the α-wollastonite and β-wollastonite and the stability of their g-values after soaking for two days confirm that the ESR signals of the β-wollastonite powder originate from the same kind of paramagnetic centers present in the α-wollastonite powder. The ESR intensity of the β-wollastonite samples increased rapidly to highest value of 5400, indicating a huge number of paramagnetic centers, but for the α-wollastonite samples, the ESR intensity decreased rapidly to 1250. The complicated behavior of the ESR signal intensity of the soaked α-wollastonite and β-wollastonite for one and two days indicates the occurrence of various types of surface reactions such as adsorption, hydration, degradation and crystallization [20]. The α-wollastonite and β-wollastonite ceramics have a high-silica content that may be soluble and develop surface hydration layer of silanols, SiOH, at the ceramic solution interface by reacting with the SBF solution [32]. The difference between the solubility of silica and crystal structure of α-wollastonite and β-wollastonite ceramics can affect the rate of silanol formation. For 3, 4 and 10 days, the g-value changed and finally decreased to 1.9189 for the β-wollastonite and 1.8670 for the α-wollastonite samples, indicating continuous variations in the chemical environments during nucleation of b-HAp. The difference between the g-value of the α-wollastonite and β-wollastonite powders after 10 days indicated that the α-wollastonite did not completely transform into HAp phase while the β-wollastonite did. The SBF solution contains various alkali ions that can form another layer containing Ca^{+2}, PO_4^{-3}, and CO_3^{+2} ions [33] by means of adsorption and rapid ion exchange. These variations in the ESR intensity values indicate that the nucleation process of b-HAp is a complex mechanism and could undergo redistribution of paramagnetic centers in the samples and could undergo molecular rearrangement of the Ca^{+2}, PO_4^{-3}, OH^- ions and H_2O molecules inside the HAp crystal lattice during the nucleation process [34]. The formation of such centers in the nucleated HAp during the soaking time is possible and there SBF solute molecules can be entrapped in the HAp lattice during HAp formation. The ESR spectrum of HAp strongly depends on several paramagnetic centers owing to the chemical structure of HAp such as OH^-, PO_4^{3-}, CO^-, O^-, O^{3-}, CO^{3-}, CO_3^{3-}, CO^{2-}, Ca^+, etc. [35–36]. The rapid reduction of the ESR signal intensity for the α-wollastonite and β-wollastonite samples probably could be explained by the fact that the amorphous nature and absence of crystallinity of induced apatite can lead to the rapid recombination of the primarily instable centers formed in the degradation/nucleation process. An increase in these ions induces the formation of amorphous carbonated hydroxyapatite layer. Increasing the soaking time results in more degradation of silica where the formed HAp layer cannot protect against the attack of the SBF solution on the surface of the α-wollastonite and β-wollastonite ceramics. The amorphous carbonated HAp layer can be crystallized by the incorporation of hydroxyl and carbonate ions that create an apatite layer [37]. These results show that the α-wollastonite and β-wollastonite powders have qualitatively different ESR spectra. Soaking samples in the SBF solution changes the

Table 1: A table showing the g-value and ESR intensity for α-WT and β-WT powder before and after soaking in SBF solution for 1, 2, 3, 4, and 10 days.

Soaking time	β-WT powder		α-WT powder	
	ESR Intensity (a.u.)	g-value	ESR Intensity (a.u.)	g-value
0d	2600 ± 60	1.9737 ± 0.0024	2000 ± 60	1.9459 ± 0.0015
1d	1900 ± 45	1.8926 ± 0.0010	2600 ± 90	1.8926 ± 0.0020
2d	5400 ± 160	1.8926 ± 0.0030	1250 ± 55	1.8926 ± 0.0010
3d	2900 ± 90	1.8670 ± 0.0029	2200 ± 100	1.8926 ± 0.0009
4d	1100 ± 55	1.8421 ± 0.0015	2200 ± 75	1.9459 ± 0.0022
10d	2950 ± 50	1.9189 ± 0.0010	1050 ± 40	1.8670 ± 0.0025

local structure of the substance owing to the nucleation of b-HAp. The ESR results have demonstrated the important role of defects for *in vitro* dissolution of wollastonite and for the formation of b-HAp. So that this study confirmed that the ESR intensity and the number of defects are related to the dissolution process of wollastonite and to the formation process of b-HAp. Hence, this study confirms that the number of defects in wollastonite may have an important role in the formation of b-HAp. Unfortunately, this study cannot detect or signify the specific role of different defect types. The results of XRD, FT-IR and ESR spectroscopy indicated that the mechanism of bioactivity of wollastonite involves the occurrence of two dependent processes: the dissolution of calcium and silicate ions from the wollastonite and the formation of b-HAp. These processes occur through the surrounding environment (SBF solution). The dissolution of wollastonite may generate increased concentrations of silica, which can work as active centers for inducing b-HAp. Precipitation and incorporation of SBF ions into these centers ensure the formation of a b-HAp layer. Any approach to control these processes will make a significant improvement to the quality of synthetic wollastonite ceramics or their composites.

IV. Conclusions

The wollastonite powders were prepared with a co-precipitation method and subsequent sintering. The α-wollastonite and β-wollastonite powders soaked in simulated body fluid (SBF) solution exhibit qualitatively different bioactivity after being soaked in SBF for various times. The wollastonite samples exhibited rapid formation of an amorphous superfine b-HAp layer after three days while β-wollastonite did this after ten days. Electron spin resonance (ESR) data showed that the formation process of b-HAp involves a complex mechanism. This mechanism involves two dependent processes; dissolution of wollastonite and formation of b-HAp. These results indicate that the α-wollastonite and β-wollastonite powders are potential candidates as bioactive ceramics for developing bone biomaterials.

References

1 Meseguer-Olmo, L., Bernabeu-Esclapez, A., Ros-Martinez, E., Sánchez-Salcedo, S., Padilla, S., Martín, A.I, Vallet-Regí, M., Clavel-Sainz, M., Lopez-Prats, F., Meseguer-Ortiz, C.L.: *In vitro* behaviour of adult mesenchymal stem cells seeded on a bioactive glass ceramic in the SiO_2-CaO-P_2O_5 system, *Acta Biomater.*, **4**, 1104 – 1113, (2008).

2 Shirazia, F.S., Mehralia, M., Oshkoura, A.A., Metselaara, H.S.C., Kadrib, N.A., AbuOsman, N.A.: Mechanical and physical properties of calcium silicate/alumina composite for biomedical engineering applications, *J. Mech. Behav. Biomed.*, **30**, 168 – 175, (2014).

3 Magallanes-Perdomo, M., Pena, P., De Aza, P.N., Carrodeguas, R.G., Rodríguez, M.A., Turrillas, X., De Aza, S., De Aza, A.H.: Devitrification studies of wollastonite-tricalcium phosphate eutectic glass, *Acta Biomater.*, **5**, 3057 – 3066, (2009).

4 Seryotkin, Y.V., Sokol, E.V., Kokh, S.N.: Natural pseudowollastonite: crystal structure, associated minerals, and geological context, *Lithos*, 134 – 135, (2012).

5 Zhang, N., Molenda, J.A., Fournelle, J.H., Murphy, W.L., Sahai, N.: Effects of pseudowollastonite ($CaSiO_3$) bioceramic on *in vitro* activity of human mesenchymal stem cells, *Biomaterials*, **31**, 7653 – 7665, (2010).

6 Magallanes-Perdomo, M., De Aza, A.H., Mateus, A.Y., Teixeira, S., Monteiro, F.J., Aza, S., Pena, P.: I*n vitro* study of the proliferation and growth of human bone marrow cells on apatite-wollastonite-2M glass ceramics, *Acta Biomater.*, **6**, 2254 – 2263, (2010).

7 Ballarre, J., Seltzer, R., Mendoza, E., Orellano, J.C., Mai, Y.W, García, C., Ceré, S.M.: Morphologic and nanomechanical characterization of bone tissue growth around bioactive sol-gel coatings containing wollastonite particles applied on stainless steel implants, *Mater. Sci. Eng.:C*, **31**, 545 – 552, (2011).

8 Aza, P.N., Guitian, F., de Aza, S.: Bioactivity of wollastonite ceramics: *In vitro* evaluation, *Scripta Metal. Mater.*, **31**, 1001 – 1005, (1994).

9 Liu, X., Ding, C.: Morphology of apatite formed on surface of wollastonite coating soaked in simulate body fluid, *Mater. Lett.*, **57**, 652 – 655, (2002).

10 De Aza, P.N., Luklinska, Z.B., Anseau, M.R., Guitian, F., De Aza, S.: Bioactivity of pseudowollastonite in human saliva, *J. Dent.*, **27**, 107 – 113, (1999).

11 De Aza, P.N., Fernández-Pradas, J.M., Serra, P.: *In vitro* bioactivity of laser ablation pseudowollastonite coating, *Biomaterials*, **25**, 1983 – 1990, (2004).

12 Habibovic, P., Barralet, J.E.: Bioinorganics and biomaterials: bone repair, *Acta Biomater.*, **7**, 3013 – 3026, (2011).

13 Carlisle, E.M.: Silicon: a possible factor in bone calcification, *Science*, 167, 279 – 80, (1970).

14 Porter, A.E., Patel, N., Skepper, J.N., Best, S.M., Bonfield, W.: Effect of sintered silicate-substituted hydroxyapatite on re-

modelling processes at the bone-implant interface, *Biomaterials*, **25**, 3303 – 3314, (2004).

15 Kokubo, T.: Surface chemistry of bioactive glass-ceramics, *J. Non-Cryst. Solids*, **120**, 138 – 151, (1990).

16 Milovac, D., Ferrer, G.G., Ivankovic, M., Ivankovic, H.: PCL-coated hydroxyapatite scaffold derived from cuttlefish bone: morphology, mechanical properties and bioactivity, *Mater. Sci. Eng.: C*, **34**, 437 – 445, (2014).

17 Norouzi, M., Garekani, A.A.: Corrosion protection by zirconia-based thin films deposited by a sol-gel spin coating method, *Ceram. Int.*, **40**, 2857 – 2861, (2014).

18 Sainz, M.A., Pena, P., Serena, S., Caballero, A.: Influence of design on bioactivity of novel $CaSiO_3$-$CaMg(SiO_3)_2$ bioceramics: *In vitro* simulated body fluid test and thermodynamic simulation, *Acta Biomater.*, **6**, 2797 – 2807, (2010).

19 Torkittikul, P., Chaipanich, A.: Optimization of calcium chloride content on bioactivity and mechanical properties of white portland cement, *Mater. Sci. Eng. C*, **32**, 282 – 289, (2012).

20 Ratner, B.D., Hoffman, A.S., Schoen, F.J., Lemons, J.E.(eds.): Biomaterials Science: An Introduction to materials in medicine. 2nd edition. Elsevier Academic Press, California, 2004.

21 Liu, X., Ding, C., Chu, P.K.: Mechanism of apatite formation on wollastonite coatings in simulated body fluids, *Biomaterials*, **25**, 1755 – 1761, (2004).

22 Sahai, N., Anseau, M.: Cyclic silicate active site and stereochemical match for apatite nucleation on pseudowollastonite bioceramic-bone interfaces, *Biomaterials*, **26**, 763 – 5770, (2005).

23 Kokubo, T., Kushitani, H., Sakka, S., Kitsugi, T., Yamamuro, T.: Solutions able to reproduce *in vivo* surface-structure changes in bioactive glass-ceramic A-W, *J. Biomed. Mater. Res.*, **24**, 721 – 734, (1990).

24 Kusrini, E., Sontang, M.: Characterization of x-ray diffraction and electron spin resonance: effects of sintering time and temperature on bovine hydroxyapatite, *Radiat. Phys. Chem.*, **81**, 118 – 125, (2012).

25 Akram, K., Ahn, J., Kwon, J.: Characterization and identification of gamma-irradiated sauces by electron spin resonance spectroscopy using different sample pretreatments, *Food Chem.*, **138**, 1878 – 1883, (2013).

26 Pattanayak, D.K., Prasad, R.C., Rao, B.T., Mohan, T.R.: Apatite wollastonite-titanium biocomposites: synthesis and in vitro evaluation, *J. Am. Ceram. Soc.*, **89**, 2172 – 2176, (2006).

27 Parida, S.K., Dash, S., Patel, S., Mishra, B.K.: Adsorption of organic molecules on silica surface, *Adv. Colloid. Interfac.*, **121**, 77 – 110, (2006).

28 Xue, W., Bandyopadhyay, A., Bose, S.: Mesoporous calcium silicate for controlled release of bovine serum albumin protein, *Acta Biomater.*, **5**, 1686 – 1696, (2009).

29 Palard, M., Champion, E., Foucaud, S.: Synthesis of silicated hydroxyapatite $Ca_{10}(PO4)_{6-x}(SiO_4)_x(OH)_{2-x}$, *J. Solid State Chem.*, **181**, 1950 – 1960, (2008).

30 Shkrob, I.A., Tadjikov, B.M., Trifunac, A.D.: Magnetic resonance studies on radiation-induced point defects in mixed oxide glasses. II. spin centers in alkali silicate glasses, *J. Non-Cryst. Solids*, **262**, 35 – 65, (2000).

31 Issa, M.A., Hassib, A.M., Dughaish, Z.H.: A study of the BaTiO,: CeO, crystal structure by EPR, *J. Phys. D: Appl. Phys.*, **1**, 2037 – 2046, (1984).

32 Park, J.: Bioceramics: Properties, characterizations, and applications. New York, Springer, 2008.

33 Hench, L.L., Wilson, J.: An Introduction to Bioceramics, Singapore. World Scientific, 1993.

34 Rokhmistrov, D.V., Nikolov, O.T., Gorobchenko, O.A., Loza, K.I.: Study of structure of calcium phosphate materials by means of electron spin resonance, *Appl. Radiat. Isotopes*, **70**, 2621 – 2626, (2012).

35 Pietak, A.M., Reid, J.W., Sayer, M.: Electron spin resonance in silicon substituted apatite and tricalcium phosphate, *Biomaterials*, **26**, 3819 – 3830, (2005).

36 Matković, I., Maltar-Strmečki, N., Babić-Ivančić, V., Sikirić, M.D., Noethig-Laslo, V.: Characterisation of β-tricalcium phosphate-based bone substitute materials by electron paramagnetic resonance spectroscopy, *Radiat. Phys. Chem.*, **81**, 1621 – 1628, (2012)

37 Boccaccini, A.R., Gough, J.E.: Tissue engineering using ceramics and polymers. Woodhead Publishing Limited, Cambridge, England, 2007.